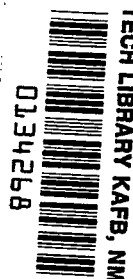


# NASA Technical Paper 1041

LOAN COPY: RET  
AFWL TECHNICAL  
KIRTLAND AFB,



## Some Physical and Thermodynamic Properties of Rocket Exhaust Clouds Measured With Infrared Scanners

Richard I. Gomberg, Andronicos G. Kantsios,  
and Frederick J. Rosensteel

NOVEMBER 1977

**NASA**



NASA Technical Paper 1041

# Some Physical and Thermodynamic Properties of Rocket Exhaust Clouds Measured With Infrared Scanners

Richard I. Gomberg, Andronicos G. Kantsios,  
and Frederick J. Rosensteel

Langley Research Center  
Hampton, Virginia



National Aeronautics  
and Space Administration

**Scientific and Technical  
Information Office**

1977

## SUMMARY

Measurements using infrared scanners were made of the radiation from exhaust clouds from liquid- and solid-propellant rocket boosters launched from the John F. Kennedy Space Center. Field measurements from four launches are discussed in this report. These measurements were intended to explore the physical and thermodynamic properties of these exhaust clouds during their formation and subsequent dispersion. In particular, information was obtained concerning the initial cloud's buoyancy, the stabilized cloud's shape and trajectory, the cloud volume as a function of time, and its initial and stabilized temperatures. Differences in radiation intensities at various wavelengths from ambient and stabilized exhaust clouds were investigated as a method of distinguishing between the two types of clouds. The infrared remote sensing method used in this study can be used at night when visible range cameras are inadequate. Infrared scanning techniques developed in this project can be applied directly to natural clouds, clouds containing certain radionuclides, or clouds of industrial pollution.

## INTRODUCTION

The launching of a solid- or liquid-propellant rocket creates a plume of hot exhaust effluents which contains such harmful species as hydrogen chloride, nitric oxide, and carbon monoxide. (See refs. 1 and 2.) These hot effluents rise because of buoyancy forces. Sometimes the products are trapped at the local inversion layer and sometimes they rise until reaching hydrostatic equilibrium with the atmosphere. In both cases, the effluents form a stabilized exhaust cloud.

To evaluate the environmental effects of rocket motor operations in the troposphere, NASA Langley Research Center has studied the behavior of these exhaust products under the Launch Vehicle Effluents program. (See refs. 3 to 6.) These measurements have shown that wind can transport the exhaust cloud for distances up to 50 km within a few hours. Consequently, it is necessary to track the exhaust cloud until dissolution to determine the effects of the exhaust products.

For a complete understanding of the dispersion of the effluents from a stabilized exhaust cloud, it is important to know the cloud's trajectory. Since the dispersion of the effluents is also affected by the growth of the exhaust cloud, it is helpful to know the cloud's volume, downwind growth rate, crosswind growth rate, and height growth rate. Under adverse weather conditions, such as haze, and during nighttime, when ordinary visual observations cannot be made, it is important to be able to obtain information about the cloud. Infrared (IR) scanners can be used to determine the cloud's trajectory and physical dimensions under adverse weather and lighting conditions.

IR scanners can also be used to study other properties of the exhaust cloud such as temperature as a function of cloud altitude. The ability of the

IR scanner to measure temperature gradients allows the strength of the buoyant forces to be determined. If the effluent cloud is extremely buoyant, it would be expected that some fraction of the effluents would penetrate any local inversion layer and disperse in the upper atmosphere. On the other hand, if the gases cool very quickly, almost all of the effluents would remain trapped below the layer for long periods of time.

In a visual range photograph, there is no easily discernible difference in appearance between an exhaust cloud and an ambient cloud. A method of quickly distinguishing, at least in a rough way, between an exhaust cloud and an ambient cloud is also desirable. IR scanners can measure temperature differences between a cloud and its surroundings, and by means of band-pass filters, they can detect spectral characteristics of clouds. These properties can possibly be used to distinguish between the two types of clouds.

In this investigation, a set of commercially available IR scanning radiometers were used to make exhaust cloud measurements during four rocket launches at the John F. Kennedy Space Center. These radiometers were sensitive to radiation emitted at wavelengths between 3 and 5.6  $\mu\text{m}$ . In addition, another scanning radiometer whose peak sensitivity was at wavelengths between 8 and 14  $\mu\text{m}$  was used. This report describes the instrumentation used and the results obtained from the four sets of field data.

Certain commercial instruments are identified in this report in order to specify adequately which instruments were used in the research effort. In no case does such identification imply recommendation or endorsement of the product by NASA, nor does it imply that these instruments are the only ones or the best ones available for the purpose. Equivalent instruments are available and would probably produce equivalent results.

#### SYMBOLS

$T_a$	ambient temperature, K
$T_{\text{plume}}$	temperature of exhaust plume, K
$t$	time of launch
$\epsilon$	emittance

#### Abbreviations:

CRT	cathode ray tube
IR	infrared
LC	launch complex

## INSTRUMENTATION

### Infrared Scanners

When a target of interest is warmer than its surroundings and its emittance is large enough so that it emits more thermal radiation than its surroundings, it can be monitored with an infrared (IR) device. IR scanners, or cameras, utilize a set of primary optics to capture the radiation, a set of moving optics (rotating prisms in this case) to collect the radiation from a particular portion of the target field, transfer optics, and a detector. (See fig. 1.) The IR detector senses the radiation and produces an output which can then be amplified. The rotating prisms produce a pulse for each rotation. These pulses, in conjunction with the detector output, are then used to produce a television-like image on an oscilloscope cathode ray tube (CRT).

In the present investigation, IR scanners with photovoltaic indium antimonide detectors were primarily used. The spectral sensitivity range of these detectors is 2 to 5.6  $\mu\text{m}$ . The lenses used degraded the overall sensitivity to 3 to 5.6  $\mu\text{m}$ . The field of view of each camera varied depending on which of several lenses was used. In most cases, a  $25^\circ$  by  $25^\circ$  field was employed, although for long-distance observations an  $8^\circ$  by  $8^\circ$  field was used. The noise equivalent temperature of the scanner is  $0.2^\circ\text{C}$  for a blackbody (a perfect emitter) at  $30^\circ\text{C}$ . The image of the emitting object is formed at a rate of 16 frames per second. This scanner can accept as many as 8 filters for band-pass measurements. The camera and supporting electronics are the AGA Thermovision System 680.

In addition to the AGA scanners, a Bofors IR scanning radiometer was also used. This unit employs an antimony-tin-telluride detector which has its peak sensitivity at wavelengths between 8 and 14  $\mu\text{m}$ . The field of view of this instrument is  $25^\circ$  in the horizontal direction but only  $12.5^\circ$  in the vertical direction. Although the frame rate of 5 per second is much slower than the AGA cameras, the Bofors camera is particularly useful because its spectral sensitivity range is different from that of the AGA units.

In order to obtain a proper exhaust cloud trajectory, the position of the centroid of the cloud as a function of time must be determined. Three scanners were usually used to track the cloud from three widely separated locations. Azimuth and elevation information from each scanner was obtained by mounting the camera on a tripod outfitted with potentiometers whose voltages provided position data. Whenever available, a special tracking unit (Askania cinetheodolite), shown in figure 2, was used (ref. 7).

### Filters

In the course of this investigation, several filters were employed with the AGA cameras. One type was a large glass filter which was held over the lens of the camera. This filter heated in hot weather, so that interpretation of data taken with it was difficult. A more satisfactory arrangement consisted of mounting several 1.27-cm-diameter filters on a holder wheel inside the housing of the camera. The holder wheel could be rotated to bring the desired filter into the

camera's field of view. These filters are not as sensitive to ambient temperature because of their proximity to a liquid nitrogen Dewar used to cool the indium antimonide detector.

Two broad-band (4.8  $\mu\text{m}$  cut-on and 3.5  $\mu\text{m}$  cut-on) and two narrow-band (3.5 to 3.7  $\mu\text{m}$  and 3.65 to 3.85  $\mu\text{m}$ ) filters were used. The broad-band transmission as a function of wavelength is given in figure 3. The narrow-band filters caused excessively small and noisy readings and so these were not useful.

### Data Display and Recording

The data were displayed on a CRT by two different methods to facilitate analysis. The first method used a gray scale with white representing the most intense signal and black the least intense. This type of display was most useful for obtaining cloud shape. The 8 to 14  $\mu\text{m}$  IR scanner had only a gray scale display. The second method of display divided the video signal into 10 discrete voltage levels. Each level was assigned a color, so that the intensity levels were color coded. This type of display was appropriate for temperature and relative intensity measurements.

An additional instrument used in conjunction with the display units was the AGA profile adapter. With this instrument, the operator could select a specific scan line at any location across the image, and a plot of the radiant intensity as a function of position along this line was displayed on a separate oscilloscope.

Data were recorded by several means. Polaroid photographs were taken of the CRT screens during tracking. In some measurements, a video tape recording of the gray scale screen was also made which provides a more complete time history of cloud formation, growth, and dimensions. In addition, an FM, 80-kHz-bandwidth, wide-band recording of the actual signals coming from one of the scanner heads was obtained. This recording is particularly valuable since the signals can be played back and analyzed with high-speed computers. In this way, spatially resolved intensity levels can be obtained.

### FIELD MEASUREMENTS

Field measurements were made of the radiation from four rocket exhaust plumes and clouds at John F. Kennedy Space Center from May 1975 to March 1976. Table I lists the four launches. These launches occurred in different weather and sunlight conditions. Launch vehicles included two Titan III's, a Delta, and an Atlas. The Titan motor's first stage uses a solid propellant, and its exhaust contains aluminum oxide particles, hydrogen chloride, and other combustion products (e.g., CO, CO<sub>2</sub>, and H<sub>2</sub>O). The Atlas uses a liquid propellant with exhaust containing water and carbon compounds. The Delta has a liquid-propellant main motor with nine "strapped on" solid-propellant boosters.

Whenever possible, three cameras at widely separated locations were used to get different views of the cloud. Table I lists the instruments and their

locations, and figure 4 is a map of the area showing the locations mentioned in the table.

## RESULTS AND DISCUSSION

### Visible and Infrared Cloud Shapes

As shown in table I, two of the measurement sets were taken in daylight conditions. Under these conditions, the plume and cloud shapes were photographed with visible range cameras. Simultaneously, the CRT screens of the infrared equipment were photographed.

Figure 5 shows photographs of visible and IR cloud shapes taken in daytime on May 22, 1975. The photograph in figure 5(a) is the cloud shape from the 3 to 5.6  $\mu\text{m}$  IR scanner. This exhaust cloud, emitted from an Atlas vehicle (liquid-propellant engine), consists primarily of water vapor and droplets, carbon dioxide, and possibly residual carbon particles. As can be seen from the figure, the shapes of the cloud in the IR photograph and in the visible range photograph are similar. All other photographs of this cloud from the liquid-propellant engine show these similarities between the visible and 3 to 5.6  $\mu\text{m}$  IR radiation. (Photographs taken from the 8 to 14  $\mu\text{m}$  IR scanner are not available for this launch.)

Similar results were obtained from the first stage of the Titan III which is fueled by a solid propellant. Its major afterburned constituents (refs. 1 and 2) include hydrogen chloride, aluminum particles, and carbon dioxide. Thus, the resultant exhaust cloud has a different composition from that of the Atlas cloud. Nevertheless, the similarities in size and shape of IR and visual images occur here also, as is evident from figure 6.

The photographs in figure 6 were taken within 1 minute of each other at about 10:25 a.m. local time on May 20, 1975. Although the field of view of the visible range camera is smaller than that of the 3 to 5.6  $\mu\text{m}$  scanning radiometer, the cloud subtends the same total angle in both pictures. The general shapes are also similar. The cloud shape from the 8 to 14  $\mu\text{m}$  IR scanner agrees with that from the visible range camera.

The obvious inference from these results is that part of the cloud's radiant transfer properties are broad band and the IR geometrical signature is the same as that given by the reflected sunlight from the cloud in the visible range. During night launches when there is no reflected sunlight, only the IR geometrical results are available. The comparisons made in this section support the assertion that the sizes and shapes measured by the infrared equipment are the sizes and shapes appropriate to the cloud.

### Rapid Cooling of Exhaust Gases

Measurements made during all of these launches consistently showed that the hot exhaust gases cool rapidly as they travel downstream of a region close to the nozzle exit plane. Figure 7(a) shows a plume in the CRT display of the 3 to

5.6  $\mu$ m IR scanner. The vehicle is a Titan III launched from LC 40 at 8:26 p.m. on March 14, 1976. This measurement was made at  $t + 12$  seconds. The intense white region at the top of the screen is the region of high-temperature afterburning. (See ref. 1.) The thinner vertical white column is the exhaust plume, and the white dot appearing at the bottom of the plume is the steel structure at the launch pad (still hot from the rocket's flames). The field of view of the picture is 3480 m wide by 3150 m high.

The horizontal white line in figure 7(a) which connects sensitivity markers 2 and 100 indicates the scan line being displayed by the profile adapter on the oscilloscope trace in figure 7(b). Ambient level signals can be seen at the extreme right and left of the picture. The extreme right side is slightly higher than the extreme left side because of an ambient cloud on the right. The plume radiation appears at the center of the picture and is easily distinguishable above the ambient level signals.

From oscilloscope traces like figure 7(b), temperature gradients are measured, and temperatures are determined by assuming the temperature of a single point in the scan line and then comparing the intensity levels of all other points in the line with this chosen point. The comparison is made by using calibration curves like those found in reference 8. In the calculation of the temperature, the emittance of the initial plume, 0.1, was taken from reference 9. Atmospheric attenuation has been accounted for by using reference 10.

The center line temperature of the plume in figure 7(a) was calculated by the method just discussed and is shown at various altitudes in figure 8. The altitude of the vehicle was roughly between 2500 and 3000 m at the time that figure 7(a) was photographed. A typical inversion height of 1500 m is indicated in figure 8. It is seen that within several seconds after launch, the temperatures within the plume below the inversion layer rapidly dropped well below the exit plane temperature of 2000 K. Rapid cooling of the gases has important physical consequences for the plume rise which has been observed to continue for a few minutes.

### Plume Rise

Although plume gases cool quickly from their peak afterburning temperatures, they still remain warmer than their surroundings. This temperature gradient causes a net upward convective current and the phenomenon of plume rise. Plume rises from rocket launches are complicated by the formation of a characteristic ring of gases at the base of the rocket plume. This ring is caused in part by the so-called flame trench and by the buoyant forces of the gases.

A flame trench is an open trench about 20 m deep reinforced by concrete. It begins under the launch pad and extends for approximately a hundred meters. This pit is sprayed with large amounts of water during an actual firing. The water cools the hot gases near the pad and helps prevent fire damage to the pad structure. As a result, the gases are channeled in a specific direction away from the pad. At the end of the trench, these gases are released, much like a horizontal smoke stack. Thus, not only is there a vertical plume but a smaller "horizontal plume" as well. When the horizontal plume rises and meets the ver-



tical column, a ring-shaped pattern evolves. This is illustrated in the photographs of figure 9 which were taken with the 3 to 5.6  $\mu\text{m}$  IR scanner of the Titan launch on March 14, 1976.

As the effluents travel far downstream of the nozzle exit plane, they slow down and the density of the plume increases. (See refs. 1 and 2.) This increase in effluent density tends to increase the effective emissivity of the plume. Thus, while the plume's emissivity near the nozzle exit plane is on the order of 0.1, it is higher during plume rise. As shown subsequently, the emittance of the stabilized cloud is expected to be near 1, so that a reasonable value for emittance during plume rise is about 0.5. With this in mind, typical temperatures of the effluents during plume rise are examined in figure 10. These measurements were taken during the Titan launch on May 20, 1975. If a value of 0.5 is assumed for emittance, each vertical unit in figure 10(b) represents 6 K. Thus, the gases shown in the profile in figure 10(b) are roughly 7 to 9 K above ambient temperature.

Although wind conditions dominate the behavior of the stabilized exhaust cloud, buoyancy forces dominate the initial plume rise. The Titan launch, on May 20, 1975, was made during an extremely calm day with light surface winds; the Titan launch on March 14, 1976, was made in heavy surface winds. Measurements taken during the two launches with the same IR scanner from the same observation site revealed nearly identical behavior of the gases during early plume rise in spite of the fact that subsequent behavior differed greatly.

Once the ring-shaped plume has formed, it rises to the stabilization altitude. Since the temperatures of the gases during plume rise are within 10 K of ambient temperature (fig. 11(b)), the rise is leisurely taking minutes to complete. The buoyancy is not sufficient to allow the cloud to penetrate any fairly strong inversion layer; if there is an inversion layer, it will be largely trapped. Since the plume rises for several minutes, any wind shears below the inversion layer can break the cloud into more than one piece. This phenomenon of multiple clouds is commonly observed; one case (March 14, 1976) is discussed in this study.

#### Radiative Properties of Stabilized Exhaust Clouds

There are two primary sources of the radiant energy emanating from the stabilized cloud that is being measured by the infrared equipment. These sources are solar radiation being reflected by the cloud and heat radiation being produced by the warm gases. To determine the relative strengths of these two sources of energy, the radiant intensity from a cloud of a Titan III taken during bright daylight was compared with that of a cloud from another Titan III launched from the same pad at night. The daylight measurement was taken on May 20, 1975, and the night measurement on March 14, 1976. Detailed meteorological information of the type found in reference 11 is available for both launches and shows that the radiative properties of the atmosphere in the two cases were not significantly different. During these two measurements, the instruments were set at high sensitivities. If the cloud were an efficient reflector of sunlight between 3 and 5.6  $\mu\text{m}$ , a large rise in intensity would

have been observed between the daylight and nighttime cases. Such a rise was not observed.

Stabilized exhaust clouds were consistently observed to block out all radiation from objects that were behind them in relation to the camera. It is inferred from this observation that the cloud is optically thick and hence, that transmission through the cloud is assumed to be small. Therefore, since reflection and transmission have been ruled out, the primary radiative phenomenon occurring in the stabilized cloud must be absorption. Since the stabilized cloud must be close to thermal equilibrium with its surroundings, the emittance value used in calculating temperature of the stabilized cloud is taken to be close to 1.

Temperatures of the stabilized exhaust clouds from the four launches were calculated from data from the 3 to 5.6  $\mu\text{m}$  IR scanner. The stabilized cloud from the Titan launch on May 20, 1975, ranged from 2 to 4 K above ambient temperature with an average signal of 3.2 K above ambient. The cloud from the night launch of the Titan on March 14, 1976, emitted at a level corresponding to between 1.4 and 2.6 K above ambient temperature with an average signal of 1.8 K. In spite of the fact that the composition of exhaust clouds from the Delta, Atlas, and Titan launches differs, the radiance levels of these clouds generally agreed. That is, the radiance from the Delta cloud (night launch) resulted in temperatures between 1.4 and 2.7 K above ambient, and the radiance from the Atlas cloud (moderate sunlight) resulted in temperatures between 3 and 4 K above ambient. Note that the daytime radiation intensities are slightly higher because of some reflected sunlight.

A fortunate incident occurred during the measurements taken of the Titan launch on March 14, 1976. An ambient cloud was in the same field of view as the exhaust cloud, so that simultaneous measurements of the intensities and spectra of radiation from natural and pollutant clouds were possible. The ambient cloud displayed a higher radiation level than the plume 1 minute after launch. As the plume formed a cloud and became optically thicker with the warm gases rising to a stabilization level, however, the radiant intensity of the exhaust cloud and natural cloud became roughly equal. For example, according to measurements taken 4 minutes after launch with the 3 to 5.6  $\mu\text{m}$  scanner, the stabilized exhaust cloud and ambient cloud were equally radiant, approximately 1.4 K above ambient temperature (fig. 11). Thus, temperature differences cannot be reliably used to distinguish between ambient and stabilized exhaust clouds.

Possible differences between the emission spectra of the ambient cloud and of the Titan III exhaust cloud were investigated. Simultaneous measurements were taken at 8:29 p.m. local time with the 3 to 5.6  $\mu\text{m}$  scanner. A measurement was made with no filter, and then a second measurement was taken with the 4.8- $\mu\text{m}$  cut-on filter. The ratio of unfiltered radiation intensity (above background intensity) of the exhaust cloud to that of the ambient cloud was about 20:19 in the 3 to 5.6  $\mu\text{m}$  band; however, with the 4.8- $\mu\text{m}$  filter this ratio was approximately 2:1. This indicates a possible prevalence of long-wavelength radiation from the exhaust cloud.

A similar measurement was carried out with the 3.5- $\mu\text{m}$  cut-on filter. With this filter, the radiation intensities from the natural and exhaust clouds

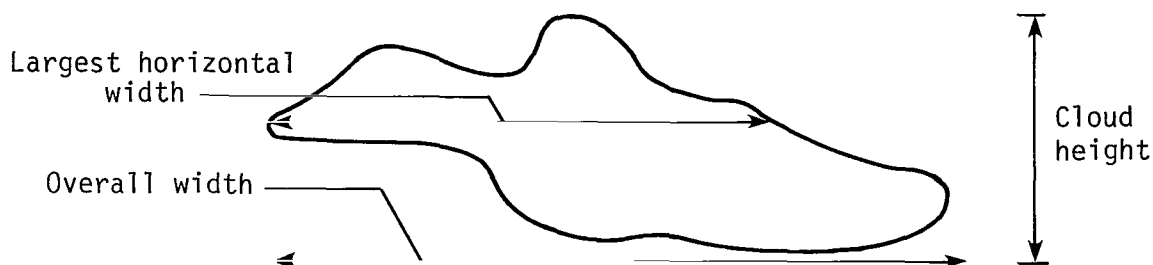
remained roughly equal although the filter slightly reduced both intensities. Since the unfiltered radiation intensities from both clouds are approximately equal and with the 4.8- $\mu\text{m}$  filter the intensity from the exhaust cloud is twice that from the ambient cloud, the ambient cloud is emitting more radiation between 3.5 and 4.8  $\mu\text{m}$  than the exhaust cloud because of the compositional differences between the two clouds.

### Cloud Trajectory and Geometry

One of the most valuable aspects of the techniques discussed in this report was the ability to track and describe the shape of exhaust clouds at night. Cloud trajectory and geometry for the Delta launch on August 26, 1975, and for the Titan launch on March 14, 1976, are discussed in this section.

Delta launch.- In figure 12, the trajectory of the Delta exhaust cloud projected along the ground is plotted, and table II gives the cloud's altitude as a function of time. Detailed wind soundings were not made during the launch. However, from movement of ambient clouds (observed from the launch pad lighted by searchlights) and from the trajectory of the ground cloud itself, a uniform wind field, indicated in figure 12, was assumed. Figure 13 gives cloud shapes for various times which were obtained from the scanner at the so-called JPL site. These cloud shapes show the development of the cloud.

In table III, the cloud's dimensions in downwind and crosswind directions are given. Listed in the table are two different measures of cloud dimension, largest horizontal width and overall width. The meaning of these two terms is illustrated in the following sketch:



The values given in table III are the averages of the measurements from the different sites. The deviation from the average is also given. Table IV gives the cloud's height as a function of time. Again, the values are averages of readings from the sites.

Table V gives the volume of the exhaust cloud as a function of time. The cloud volume includes only the gases that have collected into the compact shapes shown in figure 13. That is, the volume does not include the separate cylinders of plume gases at higher altitudes. The volume calculation was made from photographs of the CRT screen displaying the cloud. Photographs from two sites were used. The sites were chosen so that lines from them to the cloud centroid formed, as closely as possible, a right angle. The cloud was then divided into

horizontal elliptical slabs with the major and minor axis of the ellipse determined from the two photographs. The elliptical slabs were then summed over the height of the cloud and the volume was determined.

Titan launch.— The cloud from the Titan launch on March 14, 1976, was formed in the presence of a strong wind which contained at least two different shear layers at the altitudes of concern for a ground cloud. The cloud split into two pieces after approximately 3 minutes. Figure 14 presents the trajectories of these clouds, and table VI gives their altitude. The lower cloud drifted rapidly southward and dispersed after roughly 10 minutes. The larger, more stable cloud maintained a higher elevation and drifted slowly northward.

The north cloud stayed in a cigar-like shape which subsequently became very long and narrow, as shown in table VII which presents cloud dimensions. Because of the cloud's large extent, no two radiometers were able to get a view at right angles to each other. Thus, while the cloud shapes are well defined and corroborated by the different sites, the depth of the cloud in a north-south direction was not obtained by the IR instruments. Fortunately, an instrumented aircraft<sup>1</sup> made some penetration through the cloud in a north-south direction and furnished this last dimension. A reasonable estimate of the volume was made by multiplying the cross-sectional area of the cloud by the depth measured by the aircraft. This volume is presented in table VIII.

#### CONCLUDING REMARKS

Measurements with infrared (IR) scanners of radiation from rocket exhaust clouds have resulted in a set of data which is not available by other means. Since cloud shapes obtained with visible range cameras and with IR scanners agreed, it was concluded that radiation from exhaust clouds is broad band from the visible range to at least 14  $\mu\text{m}$ . Thus, cloud trajectory and shape can be determined from radiation in this wavelength range. At night when visible range cameras are unable to track the exhaust cloud, IR scanners can track the cloud and obtain cloud shape and dimensions. Successful measurements for two night launches were discussed in this report.

Temperature gradients measured with IR scanners indicate that rocket exhaust products cool rapidly after being introduced into the atmosphere. This rapid cooling causes the effluents to be trapped below any strong inversion layer and causes the plume to rise slowly. Wind shears below the inversion layer can break the slowly rising plume into multiple stabilized clouds. This phenomenon has been observed.

Radiation intensities from an ambient cloud and from an exhaust cloud were measured simultaneously with a 3 to 5.6  $\mu\text{m}$  scanning radiometer. After the exhaust cloud stabilized, it could not be distinguished from the ambient cloud by their temperatures. However, the radiation intensities from the two clouds at various wavelengths differed. These differences were probably due to com-

---

<sup>1</sup>This aircraft is part of the continuing Launch Vehicle Effluents Program carried out by the Langley Research Center (ref. 2).

positional differences between the clouds and might be used to distinguish between the two types of clouds.

Langley Research Center  
National Aeronautics and Space Administration  
Hampton, VA 23665  
September 12, 1977

#### REFERENCES

1. Stewart, Roger B.; and Gomberg, Richard I.: The Production of Nitric Oxide in the Troposphere as a Result of Solid-Rocket-Motor Afterburning. NASA TN D-8137, 1976.
2. Gomberg, Richard I.; and Stewart, Roger B.: A Computer Simulation of the Afterburning Processes Occurring Within Solid Rocket Motor Plumes in the Troposphere. NASA TN D-8303, 1976.
3. Environmental Statement for the Space Shuttle Program - Final Statement. NASA TM X-68541, 1972.
4. Gregory, Gerald L.; and Storey, Richard W., Jr.: Effluent Sampling of Titan III C Vehicle Exhaust. NASA TM X-3228, 1975.
5. Bendura, R. J.; and Crumbly, K. H.: Ground Cloud Effluent Measurements During the May 30, 1974 Titan III Launch at AFETR. NASA TM X-3539, 1977.
6. Wornom, Dewey E.; Woods, David C.; Thomas, Mitchel E.; and Tyson, Richard E.: Instrumentation of Sampling Aircraft for Measurement of Launch Vehicle Effluents. NASA TM X-3500, 1977.
7. AFETR Instrumentation Handbook. ETR-TR-71-5, U.S. Air Force, Sept. 1971. (Available from DDC as AD 735 263.)
8. AGA Thermovision 680 Operating Manual. Publ. 556.053 AGA Infrared Systems AB, c.1973.
9. Morizumi, S. J.; and Carpenter, H. J.: Thermal Radiation From the Exhaust Plume of an Aluminized Composite Propellant Rocket. J. Spacecr. & Rockets, vol. 1, no. 5, Sept.-Oct. 1964, pp. 501-507.
10. McClatchey, Robert A.; and Selby, John E. A.: Atmospheric Attenuation of Laser Radiation From 0.76 to 31.25  $\mu\text{m}$ . AFCRL-TR-74-0003. U.S. Air Force, Jan. 1974.
11. Stephens, J. Briscoe, Adelfang, S. I.; Goldford, A. I.: Compendium of Meteorological Data for the Titan III C (AF-777) Launch in May 1975. NASA TM X-73338, 1976.

TABLE I.- INSTRUMENT LOCATIONS DURING LAUNCHES

Launch vehicle	Launch complex <sup>a</sup>	Date and time of launch	Location of instruments <sup>a</sup>			
			3 to 5.6 $\mu$ m IR scanner	3 to 5.6 $\mu$ m IR scanner with filters	8 to 14 $\mu$ m IR scanner	Visible range camera
Delta	17	Aug. 26, 1975 9:43 p.m. (dark)	"JPL" site	UCS-20	UCS-26	-----
Atlas-Centaur	32	May 22, 1975 6:04 p.m. (dusk)	-----	"JPL" site	"JPL" site	"JPL" site
Titan III	40	May 20, 1975 10:04 a.m. (morning)	-----	"JPL" site	"JPL" site	"JPL" site
Titan III	40	Mar. 14, 1976 8:26 p.m. (dark)	UCS-7 and "JPL" site	VAB	VAB	

<sup>a</sup>See figure 4 for map showing launch complexes and instrument locations.

TABLE II.- ALTITUDE OF EXHAUST CLOUD FROM DELTA LAUNCH ON AUGUST 26, 1975

Time after launch, min	Altitude of cloud center, m (a)
2	393
4	711
5	729
<sup>b</sup> 6	1036
9	979
10	1020

<sup>a</sup>Error in altitude is approximately  $\pm 100$  m.

<sup>b</sup>Cloud stabilizes at an altitude of approximately 1000 m.

TABLE III.- HORIZONTAL DIMENSIONS OF EXHAUST CLOUD FROM DELTA LAUNCH

ON AUGUST 26, 1975

Time after launch, min	Largest horizontal width, m (a)		Overall width, m (a)	
	Downwind	Crosswind	Downwind	Crosswind
2	523	111	598	127
4	549	183	646	244
5	640	244	792	305
6	732	305	884	335
b <sub>9</sub>	487	366	579	548
b <sub>10</sub>	366	396	540	518

<sup>a</sup>Average of values obtained at various locations; maximum deviation of  $\pm 30$  percent.

<sup>b</sup>Cloud is dispersing.

TABLE IV.- VERTICAL DIMENSION OF EXHAUST CLOUD FROM DELTA LAUNCH

ON AUGUST 26, 1975

Time after launch, min	Cloud height, m (a)
1	258
3	442
4	671
6	841
7	909
8	756
b <sub>9</sub>	807

<sup>a</sup>Average of values obtained at various locations, deviation within  $\pm 15$  percent.

<sup>b</sup>Cloud is dispersing.

TABLE V.- VOLUME OF EXHAUST CLOUD FROM DELTA LAUNCH ON AUGUST 26, 1975

Time after launch, min	Cloud volume, km <sup>3</sup> (a)
1	0
3	.28
4	.55
6	.97
8	1.3
<sup>b</sup> 9	.92

<sup>a</sup>Error bounds are  $\pm 30$  percent.

<sup>b</sup>Cloud is dispersing.

TABLE VI.- ALTITUDE OF EXHAUST CLOUDS FROM TITAN LAUNCH ON MARCH 14, 1976

(a) North cloud

Time after launch, min	Altitude of cloud center, m
1	671
5	1037
8	1130
12	1245
<sup>a</sup> 15	1367

<sup>a</sup>Cloud stabilizes at altitude of approximately 1400 m.

(b) South cloud

Time after launch, min	Altitude, m
3	1054
6	1120
<sup>a</sup> 10	564

<sup>a</sup>Cloud is dispersing.



TABLE VII.- HORIZONTAL DIMENSIONS OF NORTH EXHAUST CLOUD

FROM TITAN LAUNCH ON MARCH 14, 1976

Time after launch, min	Largest horizontal width, m (a)		Overall width, m (a)	
	Downwind	Crosswind	Downwind	Crosswind
0.5	122	399	151	494
1.5	198	689	202	705
2.0	231	1112	248	864
8.5	744	2594	1071	3736
10.5	964	3153	1340	4380
12.5	1587	4887	1663	5119
15.0	1906	5534	1999	5807

<sup>a</sup>Average of values obtained at various locations; error bounds are  $\pm 20$  percent.

TABLE VIII.- VOLUME OF NORTH EXHAUST CLOUD FROM TITAN LAUNCH

ON MARCH 14, 1976

Time after launch, min	Cloud volume, km <sup>3</sup> (a)
0.5	0.01
2.0	.2
8.5	2.6
10.5	4.2
12.5	5.7
<sup>b</sup> 15.0	6.5

<sup>a</sup>Error bounds are  $\pm 30$  percent.

<sup>b</sup>Volume steady at 6.5 km<sup>3</sup> for next 20 minutes.

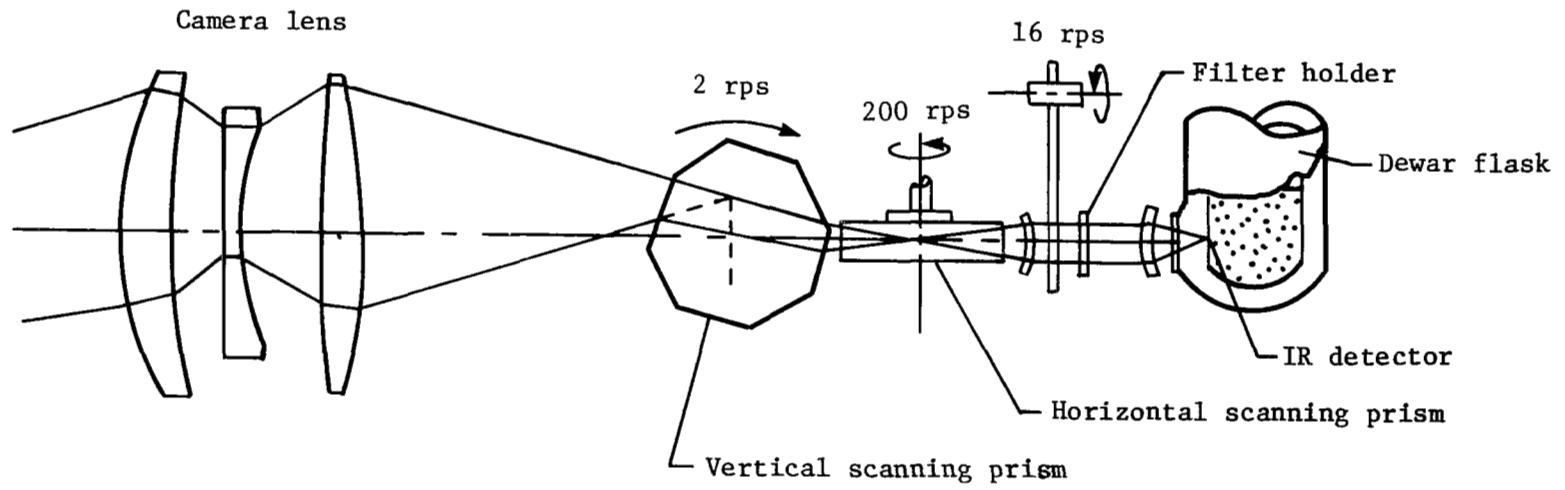
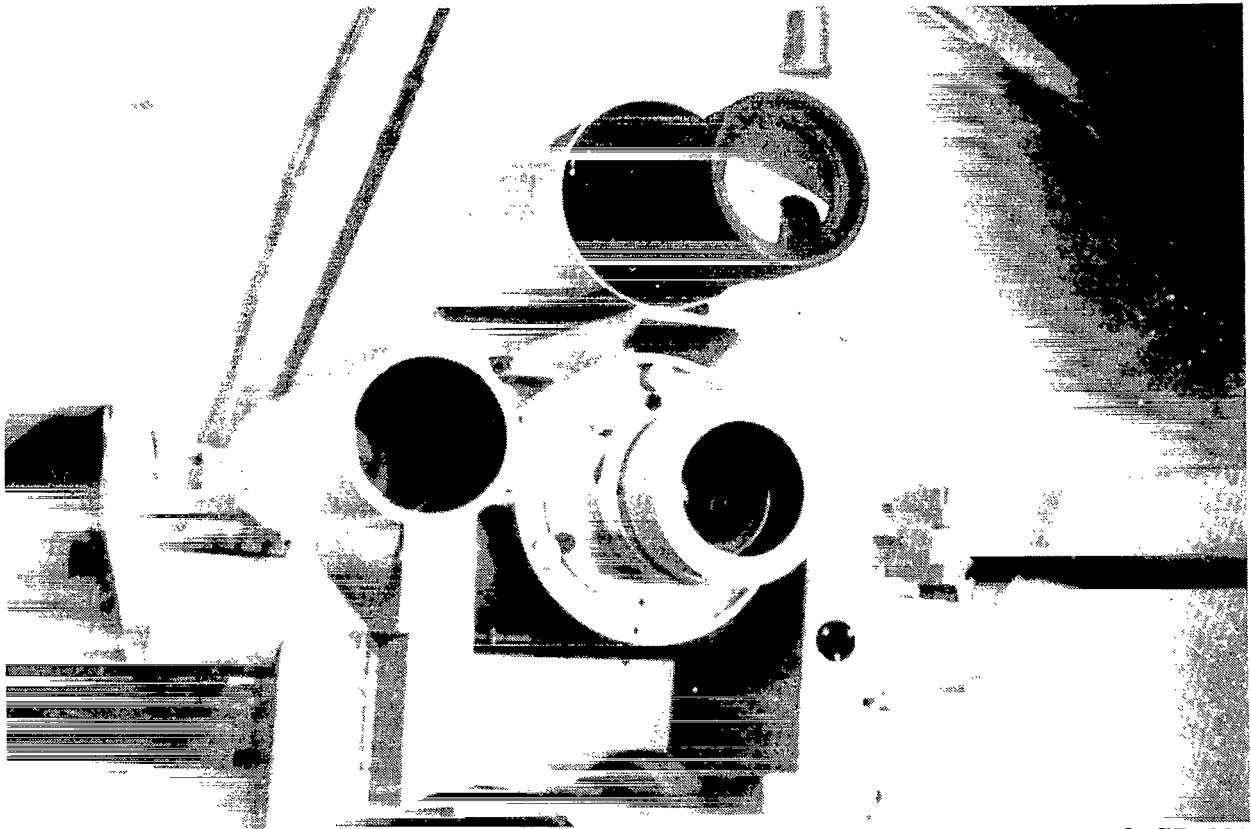
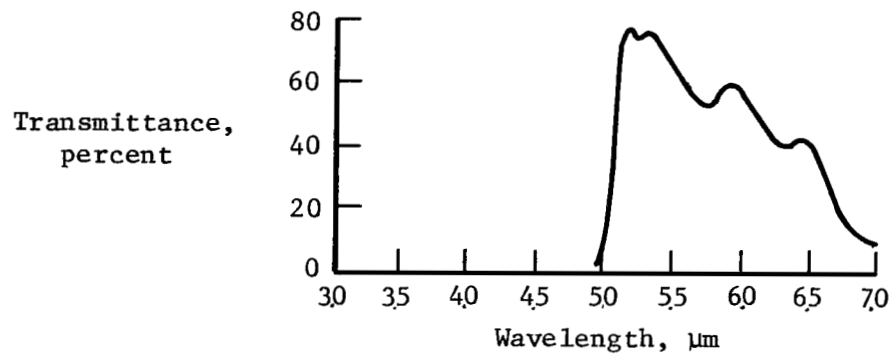


Figure 1.- Schematic diagram of IR scanner camera.

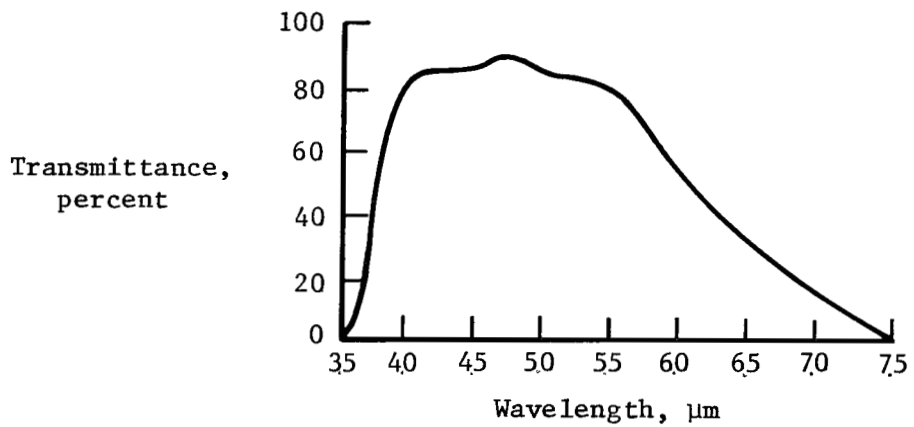


L-77-309

Figure 2.- IR camera mounted on Askania tracking device.



(a) 4.8- $\mu\text{m}$  cut-on filter.



(b) 3.5- $\mu\text{m}$  cut-on filter.

Figure 3.- Broad-band transmittance characteristics of cut-on filters.

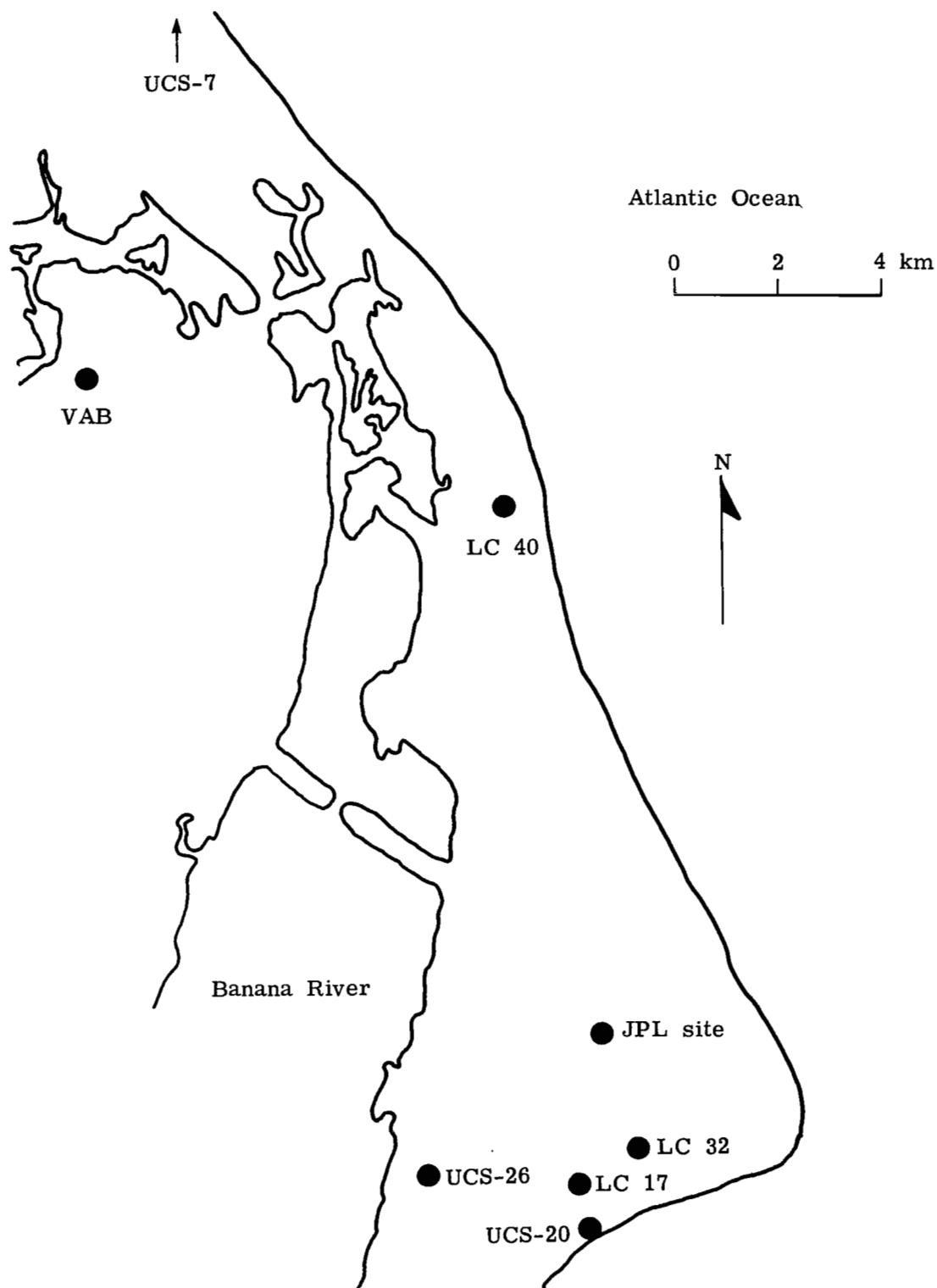
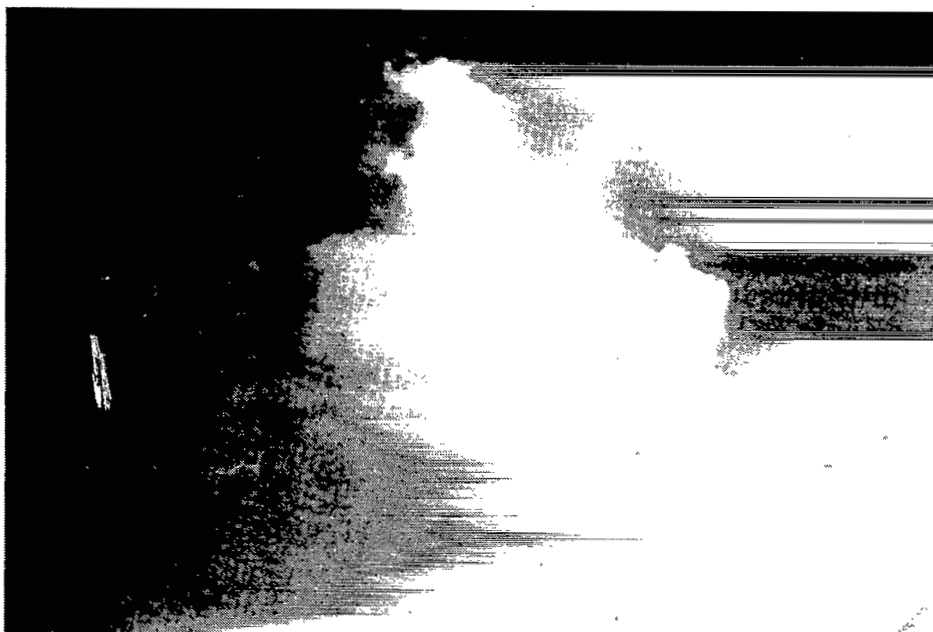
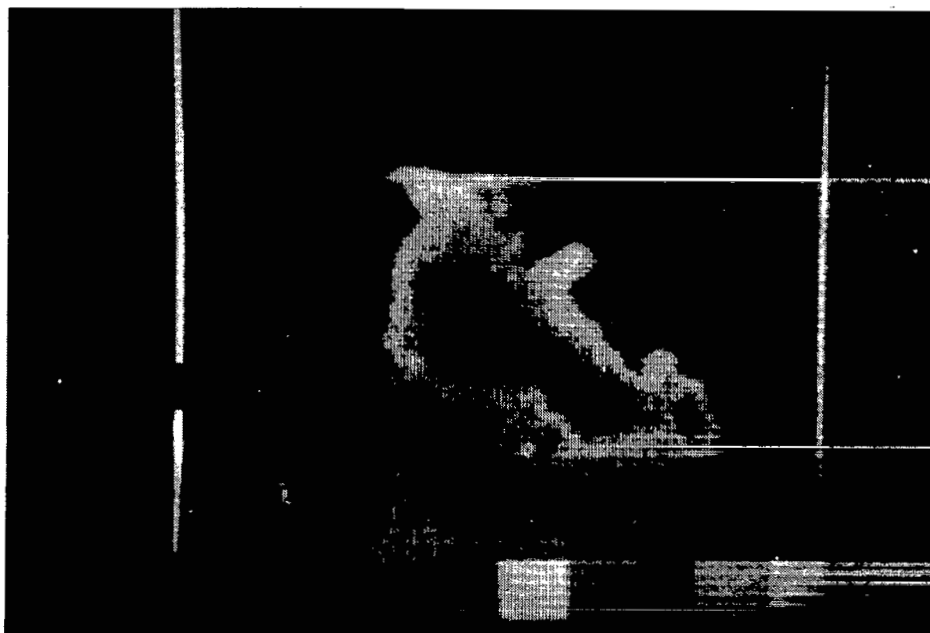


Figure 4.- Area map showing launch complexes (LC) and instrument locations.

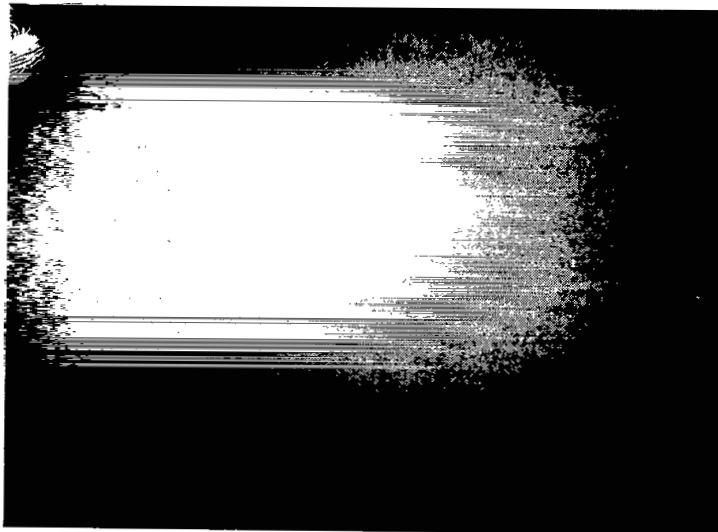


(a) Visible shape.

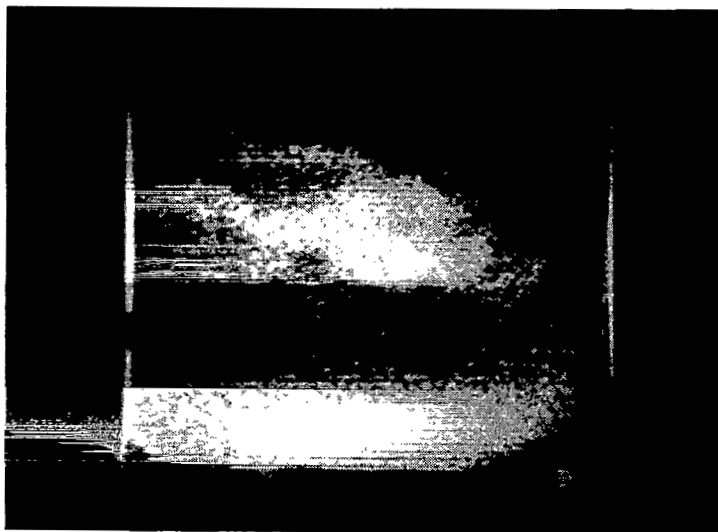


(b) IR shape.

Figure 5.- Visible and infrared cloud shapes from Atlas launch on May 22, 1975.  
Taken from JPL site at  $t + 5$  min with  $3.0$  to  $5.6 \mu\text{m}$  IR scanner.

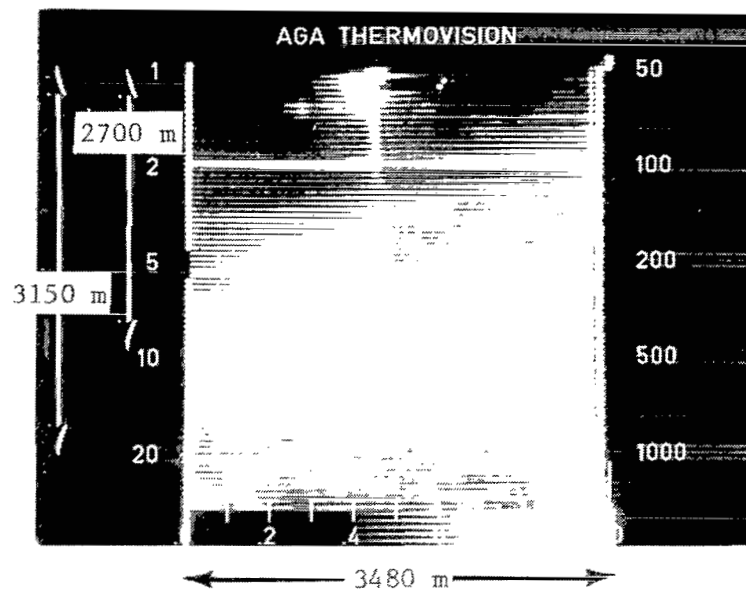


(a) Visible shape at  $t + 19$  min.

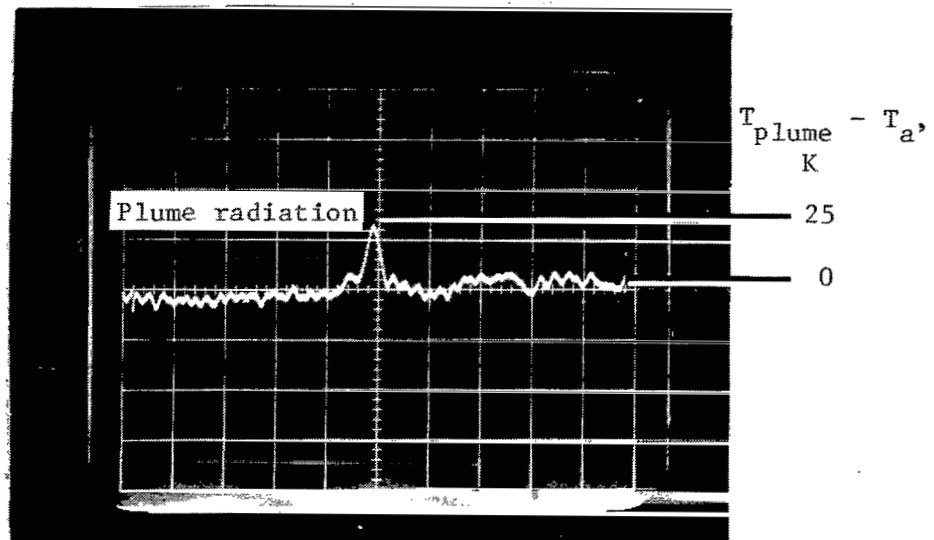


(b) IR shape at  $t + 20$  min.

Figure 6.- Visible and IR cloud shapes from Titan launch on May 20, 1975.  
Taken from JPL site with 3.0 to 5.6  $\mu\text{m}$  IR scanner.



(a) Rocket plume.



(b) Intensity analysis along white marker in figure 7(a).  $\epsilon = 0.1$ .

Figure 7.- IR radiation intensity from cloud from Titan launch on March 14, 1976. Taken from VAB site at  $t + 12$  sec with 3 to  $5.6 \mu\text{m}$  IR scanner.



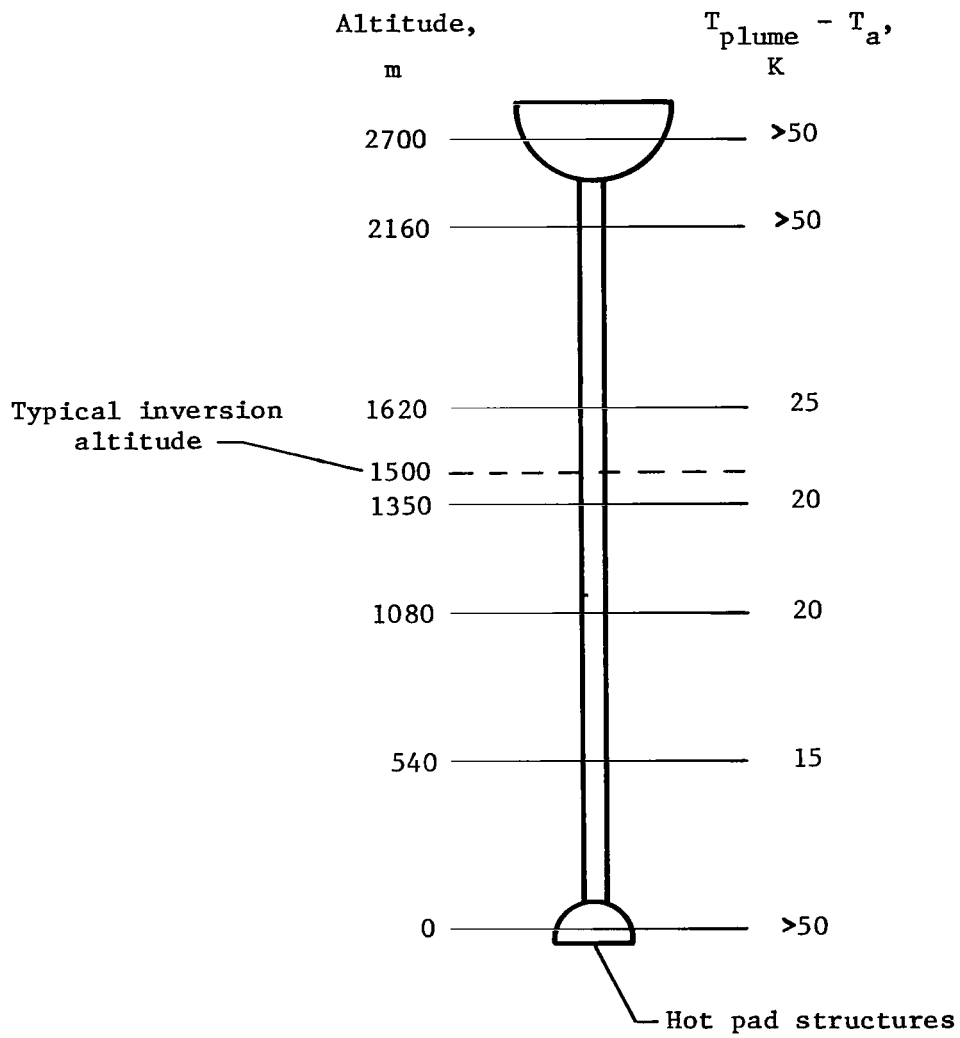
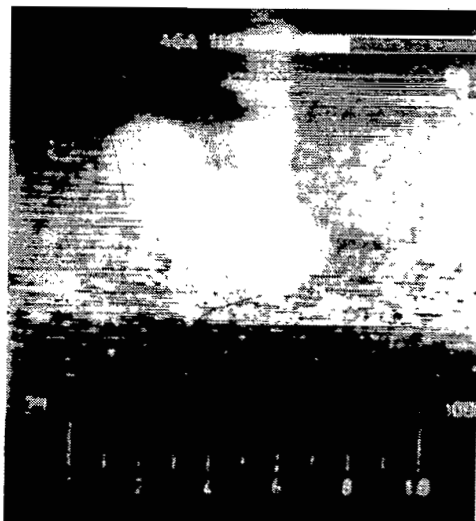
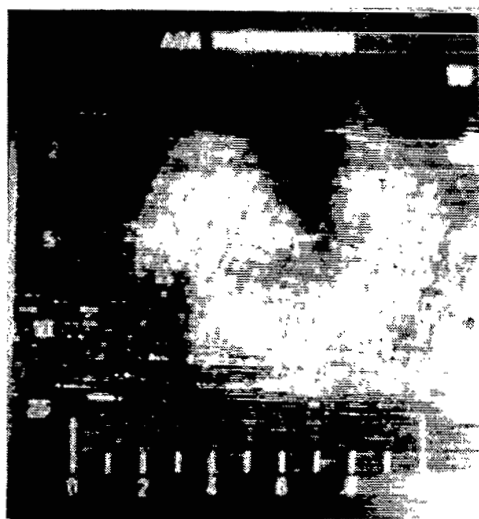


Figure 8.- Temperature analysis of figure 7(a).  $\epsilon = 0.1$ .



(a)  $t + 20$  sec.

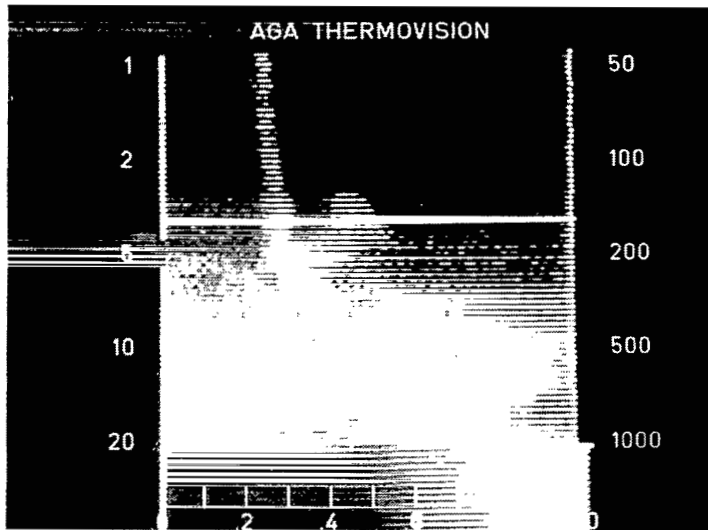


(b)  $t + 30$  sec.

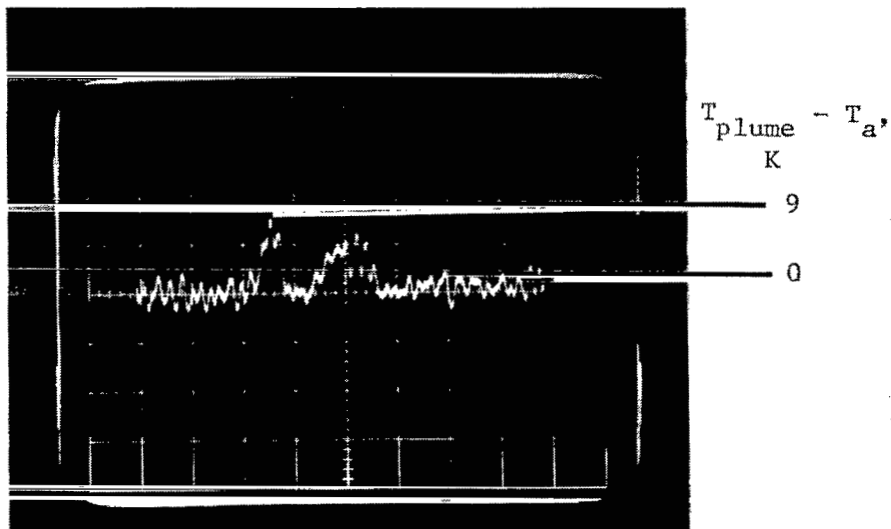


(c)  $t + 40$  sec.

Figure 9.- Development of ring-shaped plume during Titan launch on March 14, 1976. Taken from UCS-7 with 3 to 5.6  $\mu\text{m}$  IR scanner.

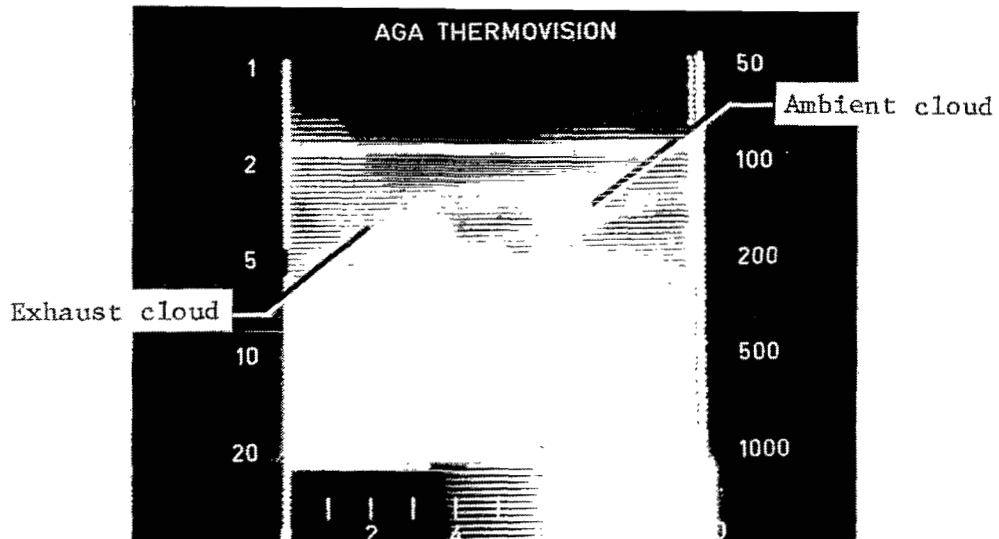


(a) Rocket plume.

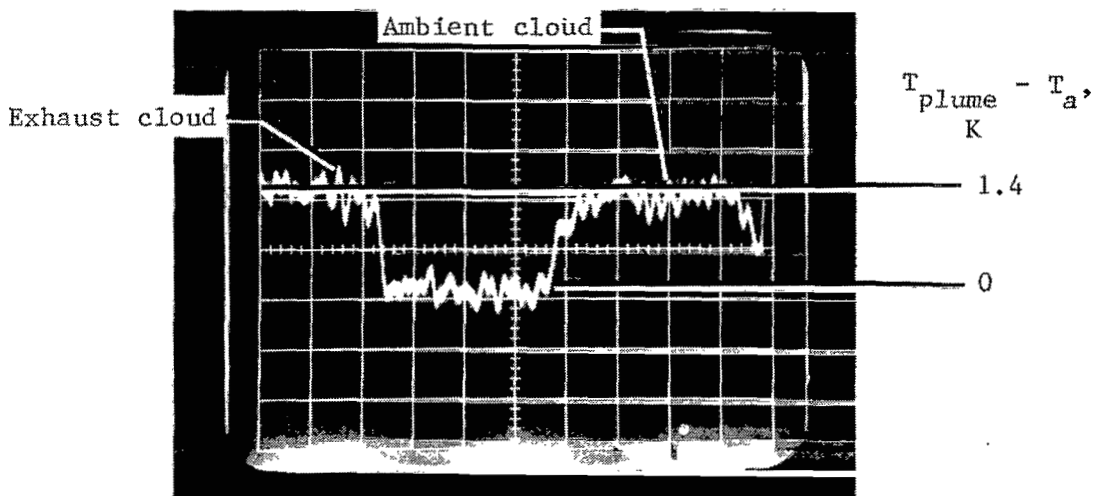


(b) Intensity analysis along white marker in figure 10(a).  $\epsilon = 0.5$ .

Figure 10.- IR radiation intensity during plume rise after Titan launch on May 20, 1975. Taken from JPL site at  $t + 20$  sec with 3 to 5.6  $\mu\text{m}$  IR scanner.



(a) Stabilized exhaust cloud and atmospheric cloud.



(b) Intensity analysis of white marker in figure 11(a).  $\epsilon = 1$ .

Figure 11.- IR radiation intensity from stabilized exhaust cloud and nearby atmospheric cloud after Titan launch on March 14, 1976. Taken from VAB site at  $t + 4$  min with 3 to 5.6  $\mu\text{m}$  IR scanner.

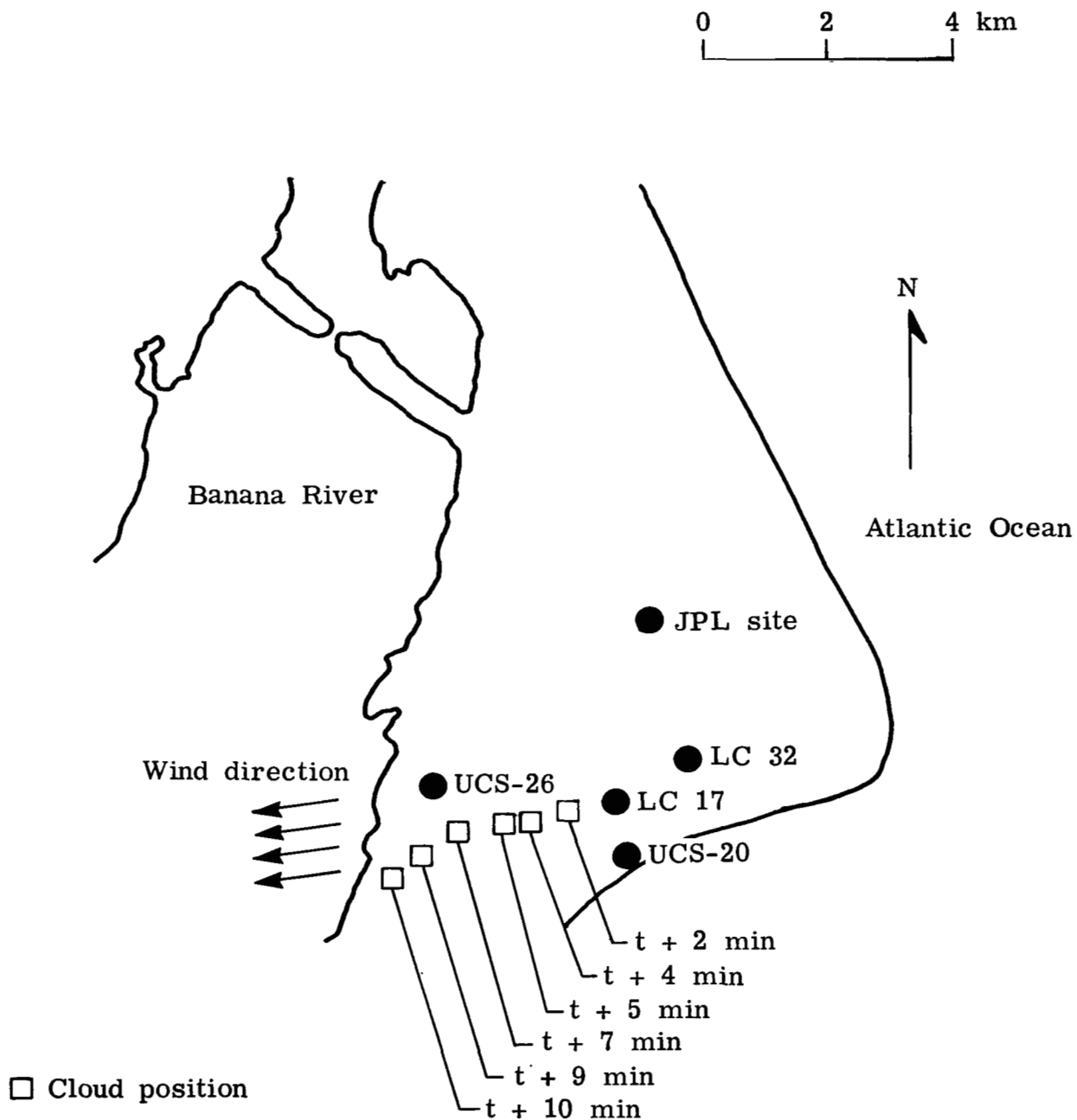
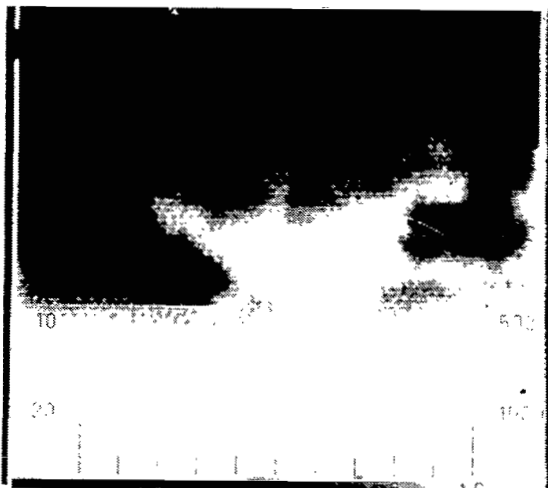


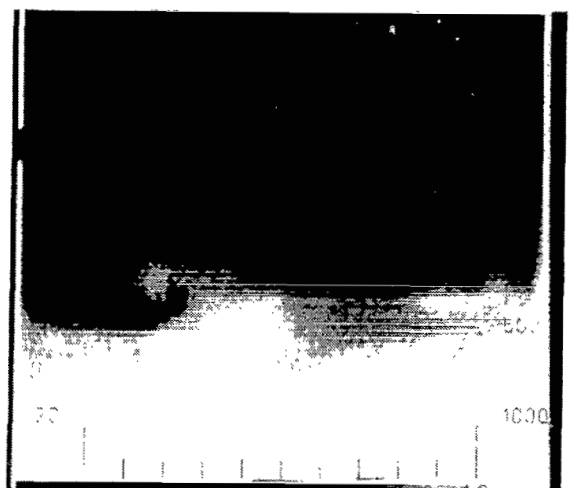
Figure 12.- Area map showing exhaust cloud trajectory after Delta launch on August 26, 1975, from LC-17.



(a)  $t + 15 \text{ sec.}$



(b)  $t + 4 \text{ min.}$



(c)  $t + 10 \text{ min.}$  Plume is dispersing.

Figure 13.- Development of exhaust cloud from Delta launch on August 26, 1975.  
Cloud shapes taken from JPL site with 3 to 5.6  $\mu\text{m}$  IR scanner.

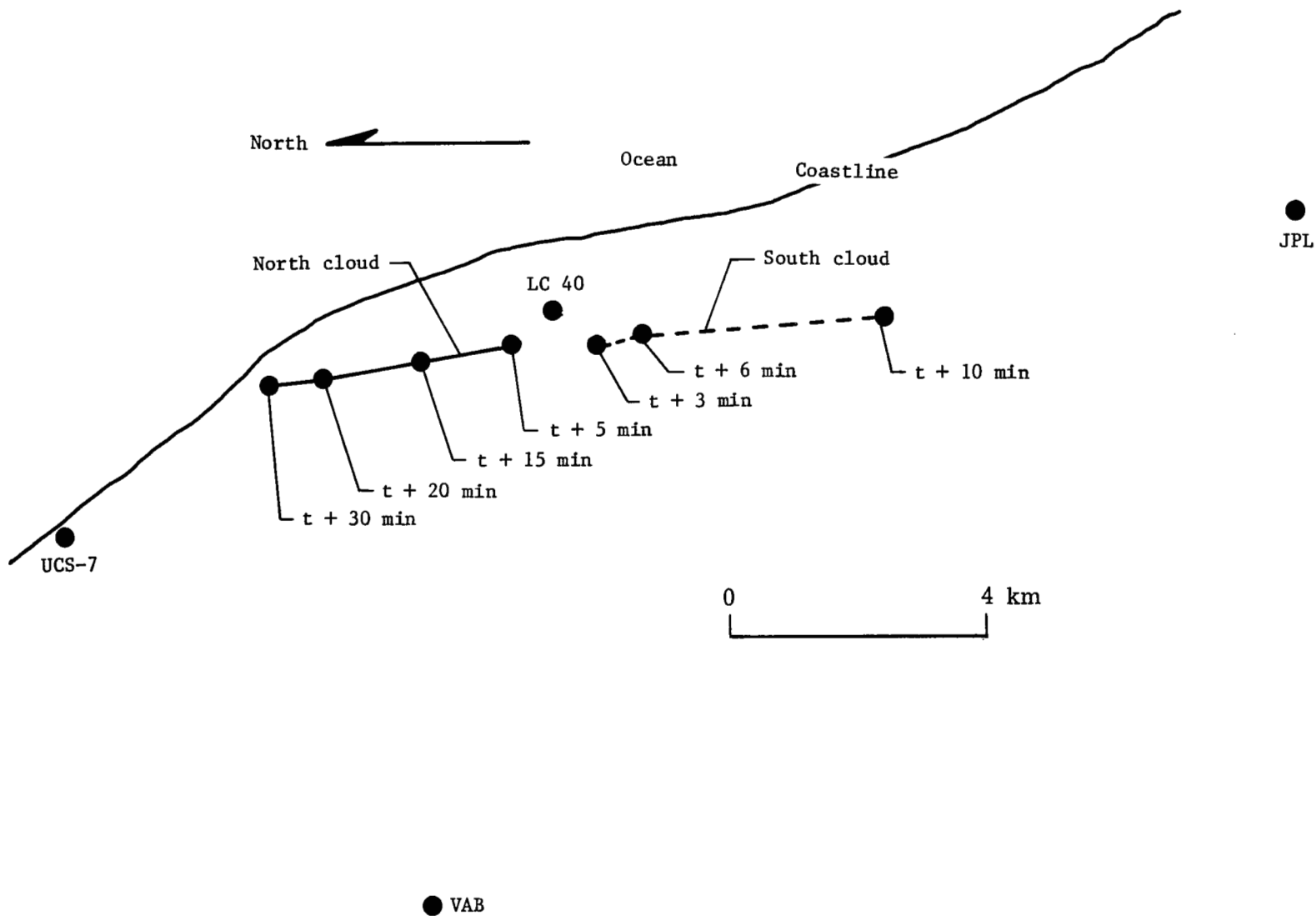


Figure 14.- Trajectories of exhaust clouds from Titan launch on March 14, 1976.

1. Report No. NASA TP-1041		2. Government Accession No.		3. Recipient's Catalog No.	
4. Title and Subtitle SOME PHYSICAL AND THERMODYNAMIC PROPERTIES OF ROCKET EXHAUST CLOUDS MEASURED WITH INFRARED SCANNERS				5. Report Date November 1977	
7. Author(s) Richard I. Gomberg, Andronicos G. Kantsios, and Frederick J. Rosensteel				6. Performing Organization Code	
9. Performing Organization Name and Address NASA Langley Research Center Hampton, VA 23665				8. Performing Organization Report No. L-11742	
12. Sponsoring Agency Name and Address National Aeronautics and Space Administration Washington, DC 20546				10. Work Unit No. 506-21-30-01	
15. Supplementary Notes				11. Contract or Grant No.	
16. Abstract <p>Measurements using infrared scanners were made of the radiation from exhaust clouds from liquid- and solid-propellant rocket boosters launched from the John F. Kennedy Space Center. Field measurements from four launches were discussed in this report. These measurements were intended to explore the physical and thermodynamic properties of these exhaust clouds during their formation and subsequent dispersion. In particular, information was obtained concerning the initial cloud's buoyancy, the stabilized cloud's shape and trajectory, the cloud volume as a function of time, and it's initial and stabilized temperatures. Differences in radiation intensities at various wavelengths from ambient and stabilized exhaust clouds were investigated as a method of distinguishing between the two types of clouds. The infrared remote sensing method used in this study can be used at night when visible range cameras are inadequate. Infrared scanning techniques developed in this project can be applied directly to natural clouds, clouds containing certain radionuclides, or clouds of industrial pollution.</p>				13. Type of Report and Period Covered Technical Paper	
				14. Sponsoring Agency Code	
17. Key Words (Suggested by Author(s)) Rocket vehicle exhaust Solid rocket motors Infrared remote sensing			18. Distribution Statement Unclassified - Unlimited  Subject Category 45		
19. Security Classif. (of this report) Unclassified	20. Security Classif. (of this page) Unclassified	21. No. of Pages 29	22. Price* \$4.00		



National Aeronautics and  
Space Administration

THIRD-CLASS BULK RATE

Postage and Fees Paid  
National Aeronautics and  
Space Administration  
NASA-451



Washington, D.C.  
20546

Official Business

Penalty for Private Use, \$300

16 1 1U,E, 093077 S00903DS  
DEPT OF THE AIR FORCE  
AF WEAPONS LABORATORY  
ATTN: TECHNICAL LIBRARY (SUL)  
KIRTLAND AFB NM 87117

**NASA**

POSTMASTER: If Undeliverable (Section 158  
Postal Manual) Do Not Return

S